Electron Transmission through Organized Organic Thin Films

R. NAAMAN*,† AND ZEEV VAGER‡

Department of Chemical Physics, Department of Particle Physics, The Weizmann Institute of Science, Rehovot 76100, Israel

Received July 30, 2002

ABSTRACT

Low-energy electron photoemission spectroscopy (LEPS) allows the study of the electronic properties of organized organic thin films (OOTF) adsorbed on conducting surfaces by monitoring the energy and angular distribution of electrons emitted from the substrate and transmitted through the film. The transmission properties are explained by electronic band structure in the organic film. This band is an example of an electron resonance that is delocalized in the layer. It results from the two-dimensional nature of the layer. Other resonances in the transmission spectra are also discussed, as well as their experimental manifestation. The temperature dependence of the electron transmission efficiency is explained in terms of dependence of the transmission probability on the initial momentum of the electron and on the relative orientation of the electron velocity and the molecules in the film. Hence, despite the fact that the molecules in the OOTF are weakly interacting, when not charged, the electron transmission through the film is governed by cooperative effects. These effects must be taken into account when considering electronic properties of adsorbed layers.

Introduction

Close-packed, organized organic layers have been the focus of substantial studies in recent years, due to their abilities to modify electronic properties of substrates,[1,2]

Ron Naaman was born in Israel, obtained his Ph.D. at the Weizmann Institute, and did his postdoctoral research at Stanford and Harvard. He is currently a Professor at the Department of Chemical Physics at the Weizmann Institute. He studies electronic properties of organized organic thin films.

Zeev Vager was born in Israel and is Professor emeritus at the Physics faculty, Department of Particle Physics, Weizmann Institute of Science. His former research subjects were structure of analogue resonances in nuclei, study of 3-D molecular structure by foil stripping Coulomb Explosion, and properties of organized organic molecular monolayers. In 1992, he was the recipient of the Rothschild's prize for the invention and applications of the Coulomb Explosion method for the study of 3-D molecular structure.

metals or semiconductors,[3-5] and applications as elements electronic devices,[6-9] light-emitting diodes,[10] sensors,[11] etc. It is usually assumed that the electronic properties of the molecules, assembled in a close packed layer, are similar to that of the isolated molecule or of the molecule embedded in an isotropic medium. The weak coupling between the neutral, ground-state molecules in a monolayer seems to support this notion and is taken as a justification for using molecular-based calculations to predict the properties of the monolayer.[12,13] However, some simple electrostatic arguments indicate that the pseudo-two-dimensional structure of the organized organic thin films (OOTF) may introduce cooperative properties that cannot be inferred from those of the isolated molecule.[14]

Here we discuss the application of low-energy photo-electron transmission spectroscopy (LEPS) as a means for investigating the electronic properties of OOTF. In a typical experiment, photoelectrons are ejected from the conductive substrate, and after being transmitted through the adsorbed layer, the energy (and or angle) dependent electrons flux is measured as a function of incident photon energy, molecular film thickness, adsorbate, and substrate types and temperature.

Electron transmission through organic thin films condensed on metal substrates has been investigated in the past mainly by low-energy electron-transmission (LEET) spectroscopy, in which single energy electrons are injected into the layer from the vacuum side and are collected on the conductive substrate.[15,16] It was suggested that for films of saturated hydrocarbon chains of various lengths, the low-energy electron transmission is governed mainly by the film's electronic band structure.[17-20] Also in the case of ordered rare gas and other simple molecular layers, the transmission[21,22] and the reflection[23] were found to correlate strongly with the band structure of the corresponding crystals. Recently, the electronic properties of adsorbed organic molecules have been investigated by two photon photoemission (TPPE) spectroscopy. Experiments have been performed both with subpicosecond[24,25] and nano-
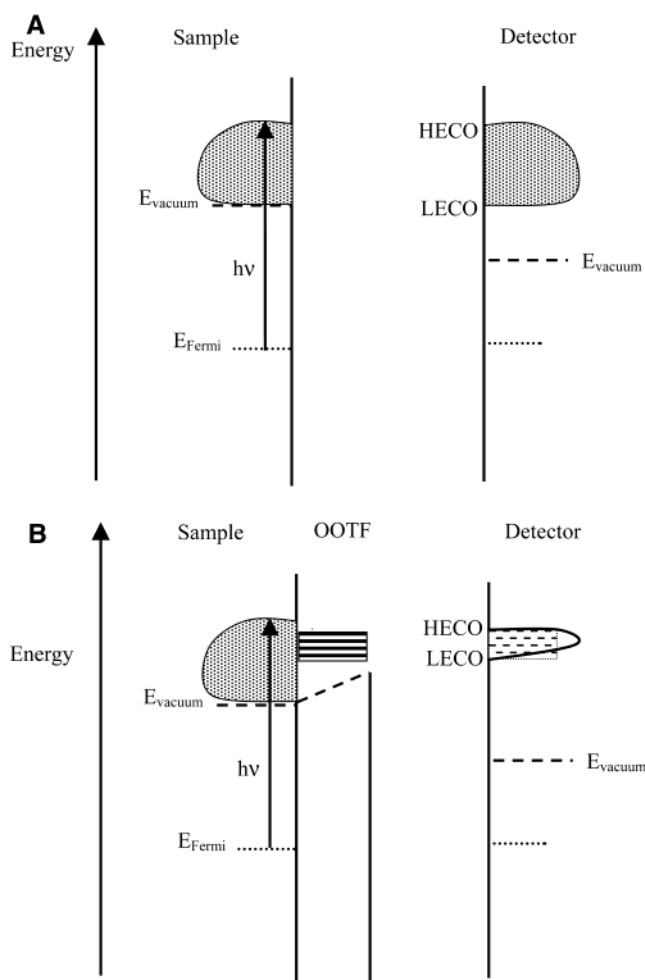
FIGURE 1. Energy-level diagram for electron transmission. The Fermi level of the system is shown as a dotted line, while the vacuum level of the sample (on the left) and the detector (on the right) are shown as dashed lines. The photoelectron energy distribution is shown for bare substrate (A) and for substrate coated with OOTF (B). The low-energy cutoff of the distribution is noted as LECO. The transmission probability through the film (B) modifies the spectrum of electrons. The high-energy cutoff (HECO) is defined by the photon energy (*hv*) and the work function of the detector and is insensitive to the substrate work function (A). The resonance states of the OOTF are shown in B as solid black-white lines.

second laser pulses.[26] In these studies, the first photon excites electrons in the substrate, which can be transferred to either a surface state or to a negative ion state on the adsorbate. A second photon detaches the electron from the metastable state and its kinetic energy and angular distribution is measured. The TPPE technique has been used to study the electronic structure of the adsorbed layer,[27] the nature of the electronic states,[28] and the effect of the thickness of the adsorbed layer.[26]

When electrons are ejected from a conductive substrate, their energy distribution, $P_0(E)$, depends on the photon energy, the density of states in the substrate, the barrier for electrons to escape from the substrate (work function), and the electron-affinity of the detector. Special attention should be given to the low- and high-energy cutoffs (LECO and HECO respectively) in the energy distribution (see Figure 1A). The LECO depends on the

work function of the substrate and the difference between it and that of the detector. The HECO is a function only of the photon energy and the electron affinity of the detector (see Figure 1A). When OOTF is adsorbed on the surface, it may change its work function by exchanging charge with the substrate or by applying force on the ejected electrons, due to the intrinsic dipole moment of the molecules on the layer. Now the LECO depends on the new work function of the metal-OOTF system (see Figure 1B). In addition, there is an energy dependent probability, $T(E)$, for electrons to be transmitted through the layer. Hence, the final energy distribution of the electrons $P(E)$ is given by

$$P(E) = P_0'(E) \cdot T(E) \qquad (1)$$

when $P_0'(E)$ is the modified energy distribution of the photoelectron ejected from the substrate, due to the chemical bonding of the OOTF. From eq 1 it is clear that in the LEPS studies $T(E)$ cannot be obtained simply by measuring $P(E)$ and the pure substrate − $P_0(E)$, since $P'_0 \neq P_0$. Still, as will be shown, LEPS provides direct information on the electronic properties of the adsorbed film.

In what follows we will discuss the mechanism that controls the electron transmission through OOTFs, the resonances expected in the energy resolved transmission, and how the dependence of the transmission on the initial direction of the electrons affects the temperature dependence of the transmission.

Experimental Section

Film Preparation and Characterization. Several type of OOTFs have been prepared, usually on 100 nm thick gold or silver films that are deposited on glass slides or silicon (100) wafers. OOTFs were deposited using either Langmuir−Blodgett (LB) or self-assembly (SA) techniques. The LB films were made from cadmium salts of arachidic [Cdar; $(CH_3(CH_2)_{18}COO^-)_2Cd^{2+}$], brassidic [Cdbr; $(CH_3(CH_2)_7CH=CH(CH_2)_{11}COO^-)_2Cd^{2+}$], or stearic [Cdst; $(CH_3(CH_2)_{16}COO^-)_2Cd^{2+}$] acids. Self-assembled films were made from octadecylmercaptane [OM; $CH_3(CH_2)_{17}SH$] and from the molecules shown in Figure 2.

The quality of the layers was determined by the transfer ratio from the trough in the case of LB films, by ellipsometric studies that probe the thickness of the layers and by IR spectroscopy. For successfully deposited films, the contact angle with water was typically 111−113°, except for the molecules shown in Figure 2, where lower angles were observed. The ellipsometric data for Cdst and Cdbr show that the thickness of each single layer is about 2.40 ± 0.05 nm, independent of the film composition. This number indicates that the Cdbr layers, despite being slightly longer than CdSt, are tilted relative to the surface normal and therefore the thickness of the layers of the two types of film are almost identical. Atomic force microscopy studies confirmed the results obtained from ellipsometry. Layers in which a 1:1 mixture of the Cdbr and Cdst were also produced and probed by the same methods, and their quality was found to be the same as
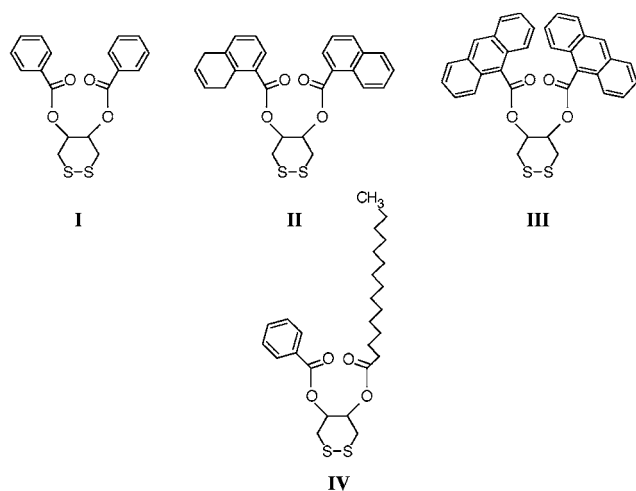
FIGURE 2. The structure of the molecules adsorbed on the gold surface.

Electron Energy

FIGURE 3. The expected electron energy distribution assuming a "classical" scattering process (dashed line). The initial photoelectron spectrum is shown as solid line.

that of the other layers.[29] From other studies,[30] it is known that the 1:1 mixed layer is homogeneous and no domains are formed.

Photoelectron Energy Distribution Measurements. The slides coated with the OOTF were attached to a temperature controlled holder and inserted into a UHV chamber pumped to below 10^{-8} mbar.[31,32] Various lasers were used to eject photoelectrons from the conducting substrate. The lasers' wavelengths were chosen so that the photon energy will be above the substrate work function, below the ionization potential of the molecules and will not be absorbed by the adsorbed film. The lasers have 10–20 ns long pulses and the pulse energy was kept below about 0.1 μJ to avoid nonlinear effects.

The laser beam is introduced into the chamber and after reflecting from the sample it exits through quartz windows. The photoelectron kinetic energy distribution was measured either via the retarding field method or by a time-of-flight electron energy analyzer. In the first method, a grid made of nickel was placed 3 mm in front of and parallel to the OOTF coated slide. The grid could be biased with a negative or positive voltage relative to the metal surface which was kept at ground potential. The close proximity of the grid and the sample ensures high collection efficiency and unperturbed collection of low energy electrons. Although the method is inherently of low resolution, it has the advantage of being sensitive to the low energy electrons. The details of the time-of-flight energy analyzer are given in ref 33. In this setup the resolution is of better than 30 meV. The electron energy distributions obtained by both methods were consistent.

The Transmission Mechanism–Electronic Band Structure. If one thinks of the electron transmission process as a random scattering process in which electrons change their momentum due to the collision with the atoms, it is expected that any initial energy distribution will become broader and some of the transmitted electrons will have lower energy than their initial energy. In the case of thick enough layers, this "relaxed" energy distribution may look as shown in Figure 3. Figure 4 presents the actual electron energy distribution of photoelectrons from gold coated
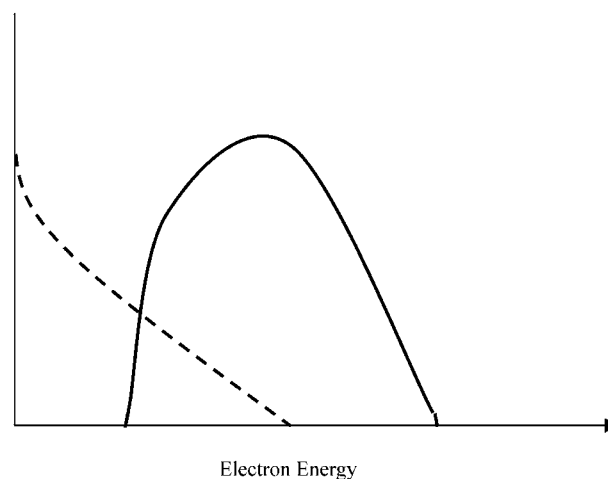
with one (A), three (B), five (C), and 13 (D) monolayers of Cdst. From the spectra shown in Figure 4A–C, it is evident the electrons energy distribution is not "relaxed". Rather it shows a high transmission probability for energies above ca. 0.8 eV and low transmission probability for electrons with lower energies. The energy distribution actually becomes narrower with increasing thickness of the layer. Only when the film becomes relatively thick (about 25 nm) does a somewhat relaxed distribution evolve (Figure 4D). The importance of film order in the electron transmission process is demonstrated in Figure 5, which presents the current density as a function of electron energy for photoelectrons transmitted through 13 layers of Cdar, before (circles) and after (squares) they were heated to 378 K and cooled back again to room temperature. Thus, before heating, electrons with energies near ca. 1 eV are transmitted through the band very efficiently with little energy loss. Following the heating, the electron energy distribution indicates that extensive random scattering processes occur.

The results presented above indicate a "nonclassical" scattering process which can in principle result from two different effects. One is related simply to the fact that thin layers exist with their thickness comparable to the electrons' wavelength, hence interferences in the transmission result in narrow peaks. These resonances are very sensitive to the thickness of the layer, but only weakly depend on the electronic properties of the molecules. Another origin for the structure in the transmission spectrum may arise from the negative ion states of the adsorbed molecules. Since the radius of the electron's orbital in these states is large, it causes coupling with nearby molecules in the layer and electronic bands are formed. In both cases the layer must be well organized.

The positions of the maxima of the distributions in Figure 4 are almost independent of the thickness of the films (1, 3, or 5 layers). This is inconsistent with narrow resonances and indicates that the second type of resonances are controlling the electron transmission. The transmission indeed depends on the film being well
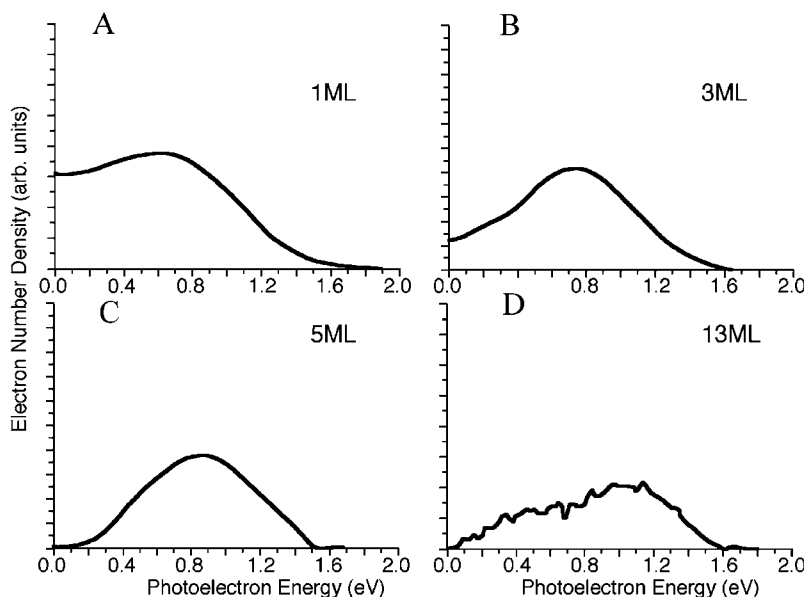
FIGURE 4. The electron energy distribution of photoelectrons from gold coated with one (A), three (B), five (C), and 13 (D) monolayers of cadmium stearate (Figure 2 from ref 49).
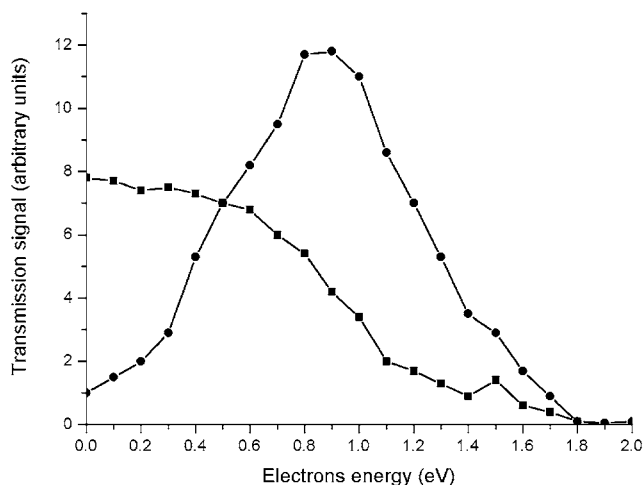

FIGURE 5. The electron energy distribution as measured by the retarding field method for photoelectrons transmitted through 13 organized (circles) and unorganized (squares) layers of Cdar (Figure 3 from ref 49).

organized, organization which is lost upon warming the layer. The same conclusion has been reached based on LEET studies, where it was suggested that for films of saturated hydrocarbon chains of various lengths, the LEET is governed mainly by the film electronic band structure.[17,18] Other LEET studies have established that the conduction band in many alkane layers is at about 0.2− 0.8 eV above the vacuum level.[20]

In the OOTF, periodicity in the potential exists both in the direction perpendicular to the layer's plane (*z*-axis) and in the directions parallel to the layer (*x,y*). In the *z* direction, the periodicity is a result of almost all the chemical functionalities being identical, CH_2 groups. The situation in the *xy* plane is different; here the periodicity results from having the molecules adsorbed in an organized layer. However, the interaction between the mol-

ecules is weak, and therefore no band structure can be observed without an additional electron.

While in a bulk solid, addition of an electron does not affect the interaction between subunits, in the OOTFs the additional electron makes all the difference. This can be understood as follows. In bulk solids, the total Hamiltonian describing the system is given by $\mathbf{H} = \Sigma h_n + \Sigma V_{nm}$, where h_n is the Hamiltonian of each subunit in the solid and V_{nm} is the interaction between the subunits. The bandwidth is characterized by V_{nm}, which in typical, nonmolecular solids, is large. When an additional electron is added to the system, it induces new interaction between the subunits, V_{nm}, and the Hamiltonian is now given by

$$H = \sum_n h_n + \sum_{n \neq m} V_{nm} + \sum_{n \neq m} V_{nm} \qquad (2)$$

Since in a typical solid $V_{nm} > V_{nm}$, the addition of an electron does not change significantly the interaction between the subunits and therefore does not affect the band structure. In OOTFs, the interaction between the subunits is weak, and therefore no band structure can be observed in the spectroscopy of the neutral system. However, when an electron is added to the system, $V_{nm} \gg V_{nm}$. Hence, the addition of the electron significantly increases the coupling between the subunits. This "electron induced coupling" results from the size of the system and its molecular properties, which forces the electron to be localized, at least in one dimension. Therefore, significant "band structure" exists only in the presence of an additional electron.

The importance of the two-dimensional periodicity on the transmission properties is demonstrated in Figure 6, which presents the transmission probability of electrons as a function of the photoelectron energy for layers of Cdar (dashed), Cdbr (dotted), and mixed layers (solid) for three (Figure 6A) and nine (Figure 6B) layers. As is clearly evident, the electron transmission through the mixed
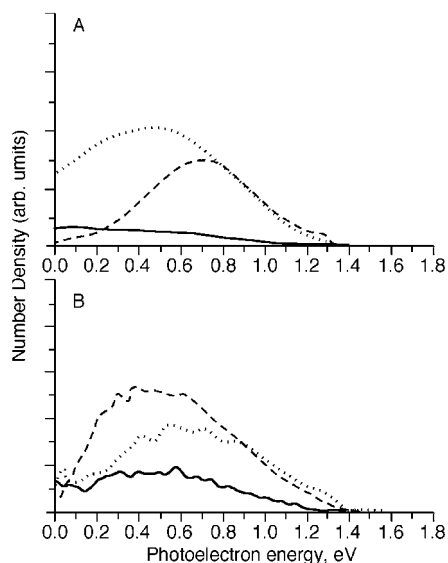
FIGURE 6. The photoelectron energy distribution is shown for electrons transmitted through layers of Cdar (dashed), Cdbr (dotted). and mixed monolayers (solid) for three (A) and nine (b) layers (Figure 2 from ref 29).

FIGURE 7. A scheme of the three possible resonances in OOTF. (i) Global resonance (A). Very weak electron-vibration interaction is expected. (ii) Localized resonances or traps (B). Usually the LEPS experiments are not detecting electrons trapped in these resonances and they appear as a reduction in the transmission probability. (iii) Quantum well structure (C). Here the electron is localized in one dimension, while it is delocalized in the other two dimensions. There is a significant electron−vibration coupling.

layers is significantly less efficient than that through the Cdar or Cdbr layers themselves. Moreover, the spectrum for the mixed layers is much closer to the relaxed type (Figure 3).

Some word of caution is needed at this point. The notion of electronic bands is of course related to the electronic structure of ordered bulk solids, and applying it to thin films is in principle questionable. Indeed, it is sufficient to associate high transmission probabilities with states of the excess electron in the film which are extended on the scale of the film thickness. In fact, numerical results[34] suggest that the correspondence with the band structure of the bulk material is substantial even for very thin films.

The results presented above indicate that "band conduction", or transmission through electronic states which are extended, is the cause of the efficient electron transmission through amphiphiles. It also rationalizes the observation that electrons are better conducted through all-trans amphiphilic chains than through chains containing some gauche bonds:[35] when the chains are in an "all-trans" configuration, the layer is ordered, and the electronic wave functions in the band are delocalized. The formation of the gauche bonds amounts to introducing disorder which increases scattering and reflection and, when pronounced enough, localizes the electronic wave function.

Resonances in Electron Transmission through OOTF. The formation of transient anion states, or electron resonances, plays an important role in low-energy electron−molecule scattering in the gas phase.[36] When electrons are transmitted through thin molecular films, the transmission probability is energy-dependent, and therefore the energy spectrum is structured.[37,38] The structure may have several origins. The broader peaks are related to the electronic band structure, as discussed above. Namely, they relate to an excess electron being delocalized
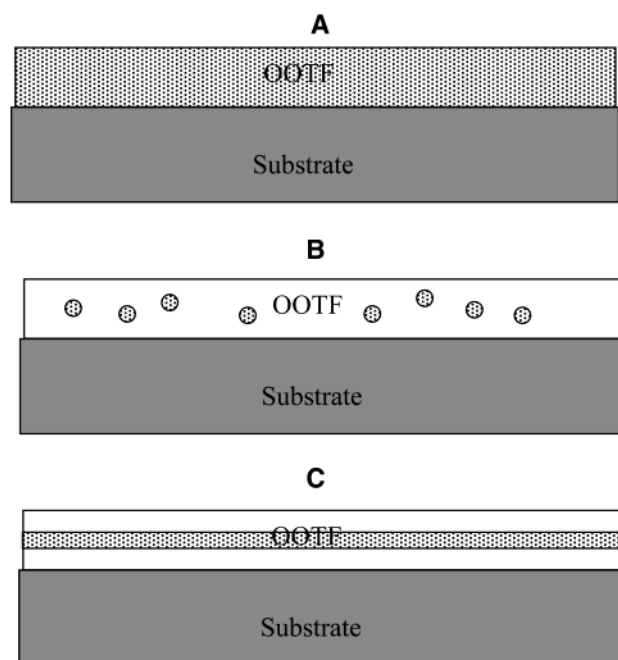
in the film and the formation of "global" states, electronic states that are delocalized over many molecules (See Figure 7A). Such resonances are expected for layers made from identical molecules containing repetitive functional groups, like the CH_2 groups in the alkyl chains.

Another type of structure may result from localized resonance states formed by either traps or impurities in the film[39] (see Figure 7B). In this case, the electrons are localized at the "trap" and due to the high charge concentration strong electron-vibration interactions exist that result in inelastic processes in the film. While these traps are observed clearly in LEET,[39] in the LEPS experiments they are manifest by reduction in the transmission probability and sometimes by charging effects, but cannot be observed as modulation on the amplitude of the spectra.

A third type of resonance may result from the two-dimensional structure of the organized organic films. In this case the electron is delocalized in two dimensions but localized in the third one (see Figure 7C).[40] Hence, the structure in the transmission probability is not a result of complete delocalization of the electron (as in the case of band structure) nor to complete localization of the electron on a single molecule (as in a typical "trap"). As expected, also in this process strong electron−vibration coupling occurs, and evidence for inelastic scattering is observed.

This type of resonance is apparent for OOTFs that were formed by self-assembling the molecules shown in Figure
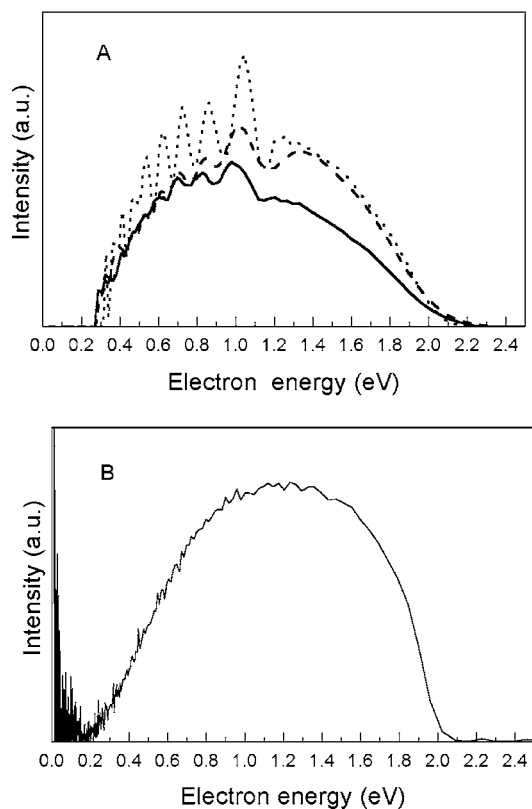
FIGURE 8. A) The electron energy distribution obtained for electrons transmitted through an organized monolayer made of molecule I (solid line) II (dashed line) and III (dotted line). The molecules are shown in Figure 2. (B) The electron energy distribution obtained for electrons transmitted through organized monolayer made of molecule IV (Figure 2) (Figures 2 and 3 in ref 50).

2 on a 100 nm polycrystalline Au film. The films were well characterized in past studies.[41] Figures 8A present the electron energy distributions obtained for electrons transmitted through films made of molecules I, II, and III (see Figure 2), while Figure 8B shows the distribution obtained for a monolayer made of molecule IV. The spectra in Figure 8A consist of two broad bands peaking at about 0.7 and 1.3 eV for all three molecules. On top of these bands, fine structure is shown, which is better resolved on the low-energy band. In the case of a benzene-substituted molecule (molecule I), a progression in the fine structure is observed with energy separation of 0.12 ± 0.01 eV. In the case of naphthalene-substituted molecules, the progression is composed from two energy intervals 0.80 ± 0.10 and 0.16 ± 0.02 eV. These results are in surprising good agreement with the vibrational resonances reported for benzene and naphthalene in the gas phase, where the resonances are at 0.123 eV for benzene and at 0.78 and 0.170 eV for naphthalene.[42] In the case of an anthracene-substituted molecule (molecule III), a long and strong anharmonic progression is observed with energy gaps of $\Delta E = 0.18, 0.15, 0.11, 0.09$, and 0.08 eV. The structure in the spectrum is more pronounced when the aromatic system becomes larger, indicating longer resonance delay for larger systems. When the aromatic rings in molecules I, II, and III were substituted by CN, NO_2, or CF_3, the sharp vibronic resonances vanish. This effect is similar to that obtained in the gas phase, where it was found that substituted aromatic do not show vibrational structure, due to breaking of the symmetry and shortening of the resonance lifetime.[42]

The observation that the fine structure in the spectra relate to the vibrational states of the anions of the aromatic parts of the molecule indicates that the extra electron is delayed near the aromatic groups and therefore electron−vibrational coupling occurs.

Figure 8A displays interference between fine structure due to vibrational coupling and a broad structure which is almost identical for the three types of monolayers. The question that arises is why such vastly different size molecules show similar broad transmission of electrons. Studies of electron scattering from these molecules in the gas phase indicated that the two first electronic resonances for benzene and naphthalene are at 1.12, 4.8 eV and 0.19, 0.9 eV, respectively. For anthracene the two first electronic resonances (above the vacuum level) are observed at about 0.6 and 1.13 eV.[42] Hence, we must conclude that despite the fact that the vibrational structure relates to the negative aromatic ions, the electronic structure, observed here, has a different origin.

In what follows we propose a model that explains all these observations. We assume that the electrons are localized on the aromatic rings, but are delocalized between the molecules, namely, that the extra electron has a state which is delocalized in the xy plane parallel to the substrate, but is localized on the Z axis (normal to the substrate) so that the extra electron wave function has high probability on the aromatic rings. Hence, the energy of the electronic states is determined by the size of the "box" in the z direction and by the polarizability of the aromatic rings.

For calculating the electronic states, the following assumptions were made:
1. We assumed boxes with a length that corresponds to the length of the aromatic rings, taking into account their tilt angle versus surface normal.
2. The energy levels of each box were downshifted by the polarization energy.

Hence, the energy levels of the systems are given by

$$E_n = \frac{n^2 h^2}{8mL^2} - \frac{\alpha e^2}{4\pi\epsilon r^4} \qquad (3)$$

where L is the length of the box, α is electronic polarizability of the aromatic system, r is the distance of the electron from the aromatic, and m and e are the mass and charge of the free electron, respectively. For $n = 1$ the expression is similar to that suggested for a polaron, and it contains the localization energy and the polarization energy.[43] However, for polarons an isotropic structure is usually assumed (L and r are taken to be the same), and the polarization contains both ionic and electronic contributions. In the present case, clearly only the electronic polarization plays any role.

The following procedure was taken in calculating the energy levels of the three different systems. In all cases

we assumed m to be the mass of a free electron. Although m is expected to be somewhat larger, this assumption does not affect substantially the results. For the benzene-substituted molecules, L and r were chosen so that the calculated states ($n = 1, 2$) coincided with the experimental observation. Then L was scaled for the naphthalene and anthracene substituted molecules by multiplying it by two and three, respectively. The polarizability (α) was assumed to be that of the aromatic groups and were taken to be 10, 16.5, and 25.4 (10^{-24} cm^3)[44] for the benzene-, naphthalene-, and anthracene-substituted molecules, respectively.

Assuming $L = 12$ Å and $r = 4$ Å, the first resonances are found to be for benzene at 0.5 and 1.8 eV, for naphthalene at 0.7 and 1.4 eV, and for anthracene at 0.9 and 1.5 eV.[45] Taking into account the fact that no fitting parameter was used in this calculation and the simplicity of the model, it is quite surprising that the results fit so well to the experimental values of about 0.7 and 1.3 eV for all three molecules. It is important to realize that the delocalization in the *xy* plane does not have to be a global one, namely on a macroscopic scale. It is enough that the scale of delocalization will be larger than a few electron wavelengths for the effect to be observed. Since the wavelength of the electrons in these experiments is on the order of 1−5 nm, it is enough to have delocalization on the scale of 50 nm to observe the effect. This scale of delocalization is important since in recent studies we observed a domain size of a few tens of nm. Hence, no macroscopic scale delocalization is required in order to observe the effect.

In the case of delocalized resonances, as shown in Figure 7A,C, it is expected that the electron transmission through the layer will depend not only on the electrons' energy but also on the initial direction of their velocity ($\vec{k}$). In this case, what will define the transmission properties is the relative orientation of the molecules and $\vec{k}$. This orientation is expected to depend on the surface temperature, since the molecules are vibrating in the plane of the layer and as a result their average tilt angle relative to the surface normal varies with temperature.

Figure 9 presents the temperature dependence of the total yield (normalized probability) of electrons transmitted through the LB film of Cdar on gold for two incident angles of the laser relative to the surface normal (80°, 9a, solid line; and 60°, 9b, solid line). A similar result was found for a Cdar film on a silicon substrate. Figure 9a shows an abrupt decrease in the photoelectron transmission yield when the surface is cooled below 300 K. The temperature effect also shows a dramatic dependence on the laser-surface incident angle. While for an incident angle of 80° the signal decreases by 80% upon cooling, for an incident angle of 60° the signal increases upon cooling. In both cases the change in the signal as function of temperature is abrupt. In addition, the change in the signal observed for an incident angle of 60° and at 80° occurs in the same temperature region. Within the experimental signal-to-noise ratio, the electron energy distribution does not vary with temperature as indicated
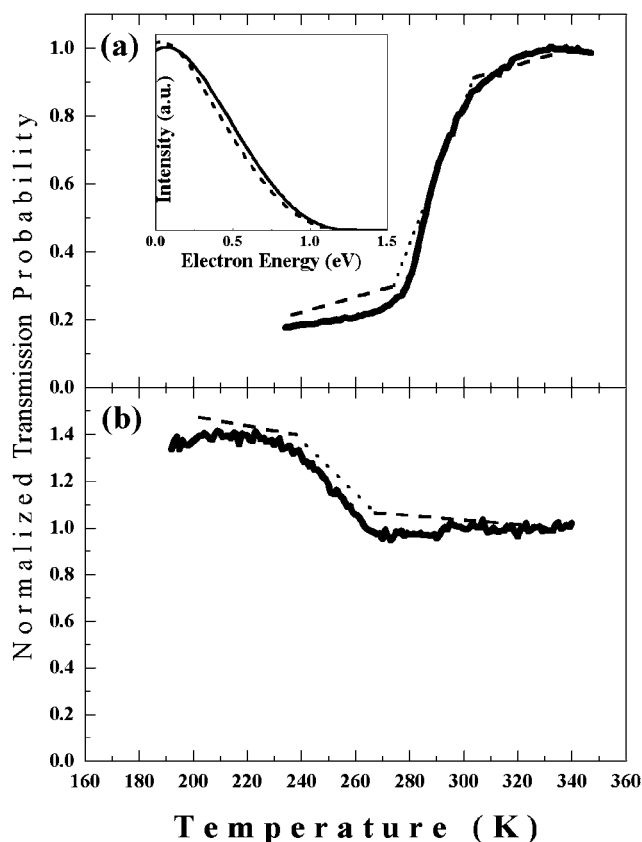

FIGURE 9. The total transmission yield as a function of temperature for a LB trilayer of Cdar on gold when the incident angle of the laser relative to the surface normal is 80 °(a) and 60°(b). The dashed lines show the results of the model calculations. The dotted lines are used only to guide the eye. The detailed model and the parameters used for the simulations are specified in ref 48. In the insert the normalized electron energy distribution is shown for surface temperatures of 303 K (solid line) and 154 K (dashed line) (Figure 2 in ref 48).

in the insert of Figure 9a, when it is presented for surface temperature of 303 K (solid line) and 154 K (dashed line). In addition, contact potential difference[46] studies performed on the film-coated substrate, at the temperature range between 350 and 200 K, indicated that there is no change in the work function as a function of temperature.

Earlier studies[47] showed a structural phase transition in LB films of Cdar over the same temperature range where the abrupt change in the photoemission occurs. Hence, the temperature dependence of the photoelectron transmission yield is correlated to structural changes in the film.

The temperature dependence of the transmission could be quantitatively modeled by assuming that it is caused by the change in orientation of molecules in the OOTF relative to the initial angular distribution of the photoelectrons.[48]

6. Summary

Transmission of electrons through organized organic thin films depends on the film's global properties, like order and alignment relative to the substrate, as well as the properties of the molecules themselves. These findings are

of importance when considering the charging/conductive properties of thin organic layers and deviate from the "classical" point of view in which a simple scattering process was assumed to operate. The LEPS technique, as applied, is a relatively simple method that extracts information on electronic properties of adsorbed films. In general, it is complementary to the more established LEET technique. In LEPS one measures the momentum distribution of the electrons after the transmission, while in LEET the momentum is defined before the transmission, but cannot be measured following the transmission process. However, by varying the light-surface incident angle and the photon energy, methods were developed for controlling, to some extent, the momentum distribution of photoelectrons also in the LEPS process. This ability allowed us to obtain information on the momentum dependent electron transmission through OOTFs.

References

(1) Ishii, H.; Sugiyama, K.; Ito, E.; Seki, K. Energy Level Alignment and Interfacial Electronic Structures at Organic/Metal and Organic/Organic Interfaces. *Adv. Mater.* **1999**, *11*, 605−625.

(2) Yaliraki, S. N.; Roitberg, A. E.; Gonzalez, C.; Mujica V.; Ratner, M. A. The injecting energy at molecule/metal interfaces: Implications for conductance of molecular junctions from an ab initio molecular description. *J. Chem. Phys.* **1999**, *111*, 6997−7002.

(3) Vilan, A.; Shanzer, A.; Cahen, D. Molecular control over Au/GaAs diodes, *Nature* **2000**, *404*, 166−168.

(4) Campbell, I. H.; Kress, J. D.; Martin, R. L.; Smith, D. L.; Barashkov, N. N.; Ferraris, J. P. Controlling charge injection in organic electronic devices using self-assembled monolayers. *Appl. Phys. Lett.* **1997**, *71*, 3528−3530.

(5) Hill, I. G.; Milliron, D.; Schwartz, J.; Kahn, A. Organic semiconductor interfaces: electronic structure and transport properties. *Appl. Surf. Sci.* **2000**, *166*, 354−362.

(6) Collier, C. P.; Wong, E. W.; Belohradsky, M.; Raymo, F. M.; Stoddart, J. F.; Kuekes, P. J.; Williams, R. S.; Heath, J. R. Electronically Configurable Molecular-Based Logic Gates. *Science* **1999** *285*, 391−394.

(7) Chen, J.; Reed, M. A.; Rawlett, A. M.; Tour, J. M. Large On−Off Ratios and Negative Differential Resistance in a Molecular Electronic Device. *Science* **1999**, *286*, 1550−1552.

(8) Vuillaume, D.; Chen B.; Metzger, R. M. Electron Transfer through a Monolayer of Hexadecylquinolinium Tricyanoquinodimethanide. *Langmuir* **1999**, *15*, 4011−4017.

(9) Punkka, E.; Rubner, R. F. Molecular heterostructure devices composed of Langmuir−Blodgett-films of conducting polymers. *J. Elect. Mater.* **1992**, *21*, 1057−1063.

(10) See for example: Yamamori, A.; Hayashi, S.; Koyama, T.; Taniguchi, Y. Transparent organic light-emitting diodes using metal acethylacetonate complexes as an electron injective buffer layer. *App. Phys. Lett.* **2001**, *78*, 3343−3345; Crone, B. K.; Davids, P. S.; Campbell, I. H.; Smith, D. L. *J. Appl. Phys.* Device model investigation of bilayer organic light emitting diodes. **2000**, *87*, 1974−1982.

(11) Wu, D. G.; Cahen, D.; Graf, P.; Naaman, R.; Nitzan, A.; Shvarts, D. Direct Detection of Low Concentration NO in Physiological Solutions by a New GaAs−Based Sensor. *Chem. Eur. J.* **2001**, *7*, 1743−1749.

(12) Nitzan A.; Benjamin, I. Electron Transmission through Molecular Layers: Numerical Simulations and Theoretical Consideration. *Acc. Chem. Res.* **1999**, *32*, 854−861.

(13) Hutchison, G. R.; Ratner, M. A.; Marks, T. J.; Naaman, R. Adsorption of polar molecules on a molecular surface. *J. Phys. Chem. B.* **2001**, *105*, 2881−2885.

(14) Vager, Z.; Naaman, R. Surprising electronic-magnetic properties of close packed organized organic layers. *Chem. Phys.* **2002**, *281*, 305−309.

(15) Sanche, L. In *Excess Electrons in Dielectric Media*; Ferradini, C., Jay-Gerin, J.-P., Eds.; CRC Press: Boca Raton, FL, 1991; Chapter 1, p 1.

(16) Sanche, L. Interaction of low-energy electrons with atomic and molecular solids. *Scanning Microsc.* **1995**, *9*, 619−656.

(17) Perluzzo, G.; Bader, G.; Caron L. G.; and Sanche, L. Direct determination of electron band energies by transmission interferences in thin films. *Phys. Rev. Lett.* **1985**, *55*, 545−548.

(18) Caron, L. G.; Perluzzo, G.; Bader, G.; and Sanche, L. Electron transmission in the energy gap of thin films of solid Ar, N_2, and *n*-hexane. *Phys. Rev. B* **1986**, *33*, 3027.

(19) Dutton, G.; Zhu, X.-Y. Electronic band formation at organic-metal interfaces: role of adsorbate−surface interaction. *J. Phys. Chem. B* **2001**, *105*, 10912−10917.

(20) (a) Maeda, T.; Miyano, K.; Sugita, K.; Ueno, N. Low energy electron transmission measurements on polydiacetylene Langmuir−Blodgett films. *Thin Solid Films* **1989**, *179*, 327−334. (b) Ueno, N.; Nakahara, H.; Sugita, K.; Fukuda, K. Electron affinity and structure of Langmuir−Blodgett films of cadmium arachidate by means of low-energy electron transmission *Thin Solid Films* **1989**, *179*, 161−170. (c) Ueno, N.; Sugita, K. Hot-electron transmission through thin amorphous films of tetratetracontane: Effects of the density of gap states on the band-gap current and its anomalous temperature dependence. *Phys. Rev. B* **1990**, *42*, 1659−1662.

(21) Bader, G.; Perluzzo, G.; Caron, L. G.; Sanche, L. Structural order effects in low-energy electron transmission spectra of condensed Ar, Kr, Xe, N_2, CO and O_2. *Phys. Rev. B* **1984**, *30*, 78.

(22) Yamane, H.; Setoyama, H.; Kera, S.; Okudaira, K. K.; Ueno, N. Low-energy electron transmission experiments on graphite. *Phys. Rev. B* **2001**, *64*, 113407.

(23) (a) Michaud, M.; Sanche, L.; Gaubert, C.; Baudoing, R. Low-energy electron reflection and transmission on Ar films condensed on polycrystalline platinum. *Surf. Sci.* **1988**, *205*, 447−464. (b) Goulet, T.; Jung, J.-M.; Michaud, M.; Jay-Gerin, J.-P.; Sanche, L. Conduction-band density of states in solid argon revealed by low-energy-electron backscattering from thin films: Role of electron mean free path. *Phys. Rev. B* **1994**, *50* 5101−5109.

(24) Ge, N.-H.; Wong, C. M.; Harris, C. B. Femtosecond studies of electron dynamics at interfaces. *Acc. Chem. Res.* **2000**, *33*, 111−118. Harris, C. B.; Ge, N.-H.; Lingle, Jr. R. L.; McNeil, J. D.; Wong, C. M. Femtosecond dynamics of electrons on surfaces and interfaces. *Annu, Rev. Phys. Chem.* **1997**, *48*, 711−744.

(25) Wong, C. M.; McNeill, J. D.; Gaffney, K. J.; Ge, N.-H.; Miller, A. D.; Liu, S. H.; Harris, C. B. Femtosecond Studies of Electron Dynamics at Dielectric-Metal Interfaces. *J. Phys. Chem. B* **1999**, *103*, 282−292.

(26) Wang, H.; Dutton, G.; Zhu, X.-Y. Electronic structure at organic/metal interfaces: Naphthalene/Cu(111). *J. Phys. Chem. B* **2000**, *104*, 10332−10338. Zhu, X.-Y. Electron transfer at molecule-metal interfaces: a two-photon photoemission study. *Annu. Rev. Phys. Chem.* **2002**, *53*, 221−247.

(27) Vondrak, T.; Cramer, C. J.; Zhu, X.-Y. The Nature of Electronic Contact in Self-Assembled Monolayers for Molecular Electronics: Evidence for Strong Coupling. *J. Phys Chem. B* **1999**, *103*, 8915−8919.

(28) Lingle, R. L., Jr.; Padowitz, D. F.; Jordan, R. E.; McNeill, J. D.; Harris, C. B. Two-dimensional localization of electrons at interfaces. *Phys. Rev. Lett.* **1994**, *72*, 2243−2246.

(29) Kadyshevitch A.; Ananthavel S. P.; Naaman R. The role of three-dimensional structure in electron transmission through thin organic layers. *J. Chem. Phys.* **1997**, *107*, 1288−1290.

(30) Popovitz-Biro, R.; Wang, J. L.; Majewski, J.; Shavit, E.; Leiserovitch, L.; Lahav, M. Induced freezing of supercooled water into ice by self-assembled crystalline monolayers of amphiphilic alcohols at the air−water interface. *J. Am. Chem. Soc.* **1994**, *116*, 1179−1191.

(31) Kadyshevitch A.; Naaman R. Photoelectron transmission through organized organic thin films. *Phys. Rev. Lett.* **1995**, *74*, 3443−3446.

(32) Kadyshevitch A.; Naaman R. The interactions of electrons with organized organic films studied by photoelectron transmission. *Thin Solid Films* **1996**, *288*, 139−146.

(33) Naaman, R.; Haran, A.; Nitzan, A.; Evans, D.; Galperin, M. Electron transmission through molecular layers. *J. Phys. Chem. B* **1998**, *102*, 3658−3668.

(34) Haran, A.; Kadyshevitch, A.; Cohen H.; Naaman, R.; Evans, D.; Seidman, T.; Nitzan, A. Electron transmission through band structure in organized organic thin films. *Chem. Phys. Lett.* **1997**, *268*, 475−480.

(35) Haran, A.; Waldeck, D. H.; Naaman, R.; Moons E.; and Cahen, D. The dependence of electron-transfer efficiency on the conformational order in organic monolayers. *Science* **1994**, *263*, 948−950.

(36) Jordan, K. D.; Burrow, P. D. Temporary anion states of polyatomic hydrocarbons. *Chem. Rev.* **1987**, *87*, 557−588 and references therein.

(37) Palmer, R. E.; Rous, P. J. Resonances in electron scattering by molecules on surfaces. *Rev. Mod. Phys.* **1992**, *64*, 383−440.

(38) Sanche, L. Low-energy electron scattering from molecules on surfaces. *J. Phys. B* **1990**, *23*, 1597−1624.

(39) For example, see: Michaud, M.; Lepage, M; Sanche, L. Lifetime of negative ion resonances and density of free electron states: O$_2$ isolated in an argon matrix, *Phys. Rev. Lett.* **1998**, *81*, 2807−2810 and references therein.

(40) McNeill, J. D.; Lingle, Jr., R. L.;. Jordan, R. E.; Padowitz, D. F.; Harris, C. B. Interfacial quantum well states of Xe and Kr adsorbed on Ag(111). *J. Chem. Phys.* **1996**, *105*, 3883−3891.

(41) Bruening, M.; Cohen, R.; Guillemoles, J. F.; Moav, T.; Libman, J.; Shanzer, A.; Cahen D. Simultaneous Control of Surface Potential and Wetting of Solids with Chemisorbed Multifunctional Ligands. *J. Am. Chem. Soc.* **1997**, *119*, 5720−5728.

(42) Burrow, P. D.; Michejda J. A.; Jordan, K. D. Electron transmission study of the temporary negative ion states of selected benzenoid and conjugated aromatic hydrocarbons. *J. Chem. Phys.* **1987**, *86*, 9−24.

(43) Cox, P. A. *The electronic Structure and Chemistry of Solids*; Oxford University Press: Oxford, 1987; p 179.

(44) *Hand Book of Chemistry and Physics*, 78th ed.; Lide, D. R., Ed.; CRC Presss: Boca Raton, FL, 1997.

(45) Only states with positive energy were taken into account, since the photoelectrons energy is above the vacuum level. For naphthalene- and anthracene-substituted molecules, resonances at 0.1 and 0.4 eV were also calculated, but since no electrons at these energies were detected, it is not possible to compare these results with the experimental observations.

(46) Surplice, N. A.; D'Arcy, R. J. A critique of the Kelvin method of measuring work functions. *J. Phys. E: Sci. Instrum.* **1970**, *3*, 477−482.

(47) Paz, Y.; Trakhtenberg, S.; Naaman, R. Phase-transition in organized organic thin-films as detected by their reactivity. *J. Phys. Chem.* **1993**, *97*, 9075−9077; The reaction between O(^{3}P) and organized organic thin film, *J. Phys. Chem.* **1994**, *98*, 13517−13523.

(48) Haran, A.; Dimitrov, D.; Trakhtenberg, S.; Naaman, R. Temperature dependence of electron transmission through organized organic thin films. *J. Chem. Phys.* **2000**, *113*, 7571−7577.

(49) Kadyshevitch, A.; Naaman, R. Electron transmission through thin organized organic films. *Surf. Interface Anal.* **1997**, *25*, 71−75.

(50) Ray, K.; Shanzer, A.; Waldeck, D. H.; Naaman, R. Resonances in low-energy electron transmission through organized organic films: Evidence for molecular quantum well. *Phys. Rev. B* **1999**, *60*, 13347−13350.

AR010008T